

Coherent Soft-X-Ray Dynamic Light Scattering from Smectic-A Films

A. C. Price,¹ L. B. Sorensen,¹ S. D. Kevan,² J. Toner,² A. Poniewierski,³ and R. Holyst³

¹Physics Department, University of Washington, Seattle, Washington 98195

²Physics Department, University of Oregon, Eugene, Oregon 97403

³Institute of Physical Chemistry and College of Science, Polish Academy of Sciences, Warsaw, Poland

(Received 28 April 1998)

We have used coherent soft-x-ray dynamic light scattering at the Bragg peak to measure the thermally driven layer fluctuations in freely suspended films of five different smectic-A liquid crystals: 4O.8, 7O.7, 8CB, 8OCB, and 10OCB. The measured relaxation times at a scattering wave vector corresponding to the interlayer spacing ($2\pi q^{-1} \approx 30 \text{ \AA}$) ranged from 2 to 60 μs for films from 4 to 50 μm thick. Thus, we have achieved the same time resolution as conventional laser dynamic light scattering, but with 100 times higher spatial resolution. [S0031-9007(98)08149-6]

PACS numbers: 61.30.-v, 42.25.Kb, 61.10.Eq

How can we study the thermally driven fluctuations of molecules? Can we use the x-ray analog of conventional laser dynamic light scattering? By providing coherent light, the laser revolutionized infrared, visible, and ultraviolet optics. What will be the impact of the new coherent x-ray sources? More specifically, what will we learn using dynamic light scattering (DLS) with coherent x rays? These questions are currently being addressed in the hard-x-ray regime [1–4]. In this Letter, we show that we can use the *soft-x-ray* analog of laser light scattering to study the thermally driven layer fluctuations of the molecules in a smectic-A (SmA) liquid crystal film, and that we can obtain the same time resolution (about 1 μs) as conventional laser light scattering, but with 100 times better spatial resolution.

The recent hard-x-ray experiments have been used to study fluctuations on time scales from tenths of a second to hours using x-ray wavelengths near 1 \AA [1–4]. We have chosen to develop soft-x-ray DLS, with wavelengths in the range 10 to 100 \AA , in order to study microsecond fluctuations, for the following two main reasons: (1) Soft x rays have sufficiently small wavelengths for the study of systems where the length scales of interest are molecular sizes as opposed to atomic sizes, and (2) a soft-x-ray source can provide more coherent flux than a hard-x-ray source of equivalent brightness. The available coherent flux from an incoherent source, such as a synchrotron source, is given by [5]

$$I_{\text{coh}} = B \left(\frac{\lambda}{2} \right)^2 \left(\frac{\Delta E}{E} \right). \quad (1)$$

Here B is the spectral brightness, λ is the wavelength, and $\Delta E/E$ is the energy resolution. Since all third generation hard-x-ray and soft-x-ray sources are of comparable brightness [6], this implies that at our soft-x-ray wavelength, $\lambda = 44 \text{ \AA}$, as compared with a hard-x-ray wavelength, $\lambda = 1 \text{ \AA}$, we can get about $44^2 \approx 1900$ times more coherent x-ray flux with the same fractional energy resolution.

Our experiments were performed using the undulator Beamline 7 at the Advanced Light Source at Lawrence

Berkeley National Laboratory. In Fig. 1, a schematic of our experiment is given, showing the undulator source, monochromator, beam line optics, and our vacuum chamber. Between the undulator source and our end station, the beam passes first through a spherical grating monochromator ($\Delta E/E \approx 10^{-4}$), and then through beam line optics consisting of focusing mirrors and a multilayer reflector. The multilayer reflector, with 10% reflectivity, was used to direct the beam away from the beam line's permanent end stations and towards our experiment. Spatially coherent soft x rays were generated by passing the incoherent beam through a double pinhole spatial filter located within our vacuum chamber. The coherent beam was then scattered from a freely suspended SmA film in the Bragg geometry. The Bragg reflected light, produced by the layered structure of the liquid crystal, and the transmitted beam were monitored by separate detectors.

In order to perform a coherent scattering experiment, the following two conditions must be met: (1) The incident beam must be spatially, or transversely, coherent, and (2) the maximum path length difference introduced by the scattering medium must be less than the longitudinal coherence length. The first condition is satisfied by choosing pinhole diameters and separations which satisfy $P_2 = \lambda L/2P_1$, where P_1 and P_2 are the diameters of the first and

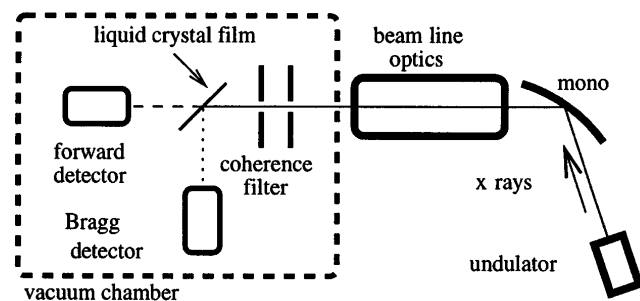


FIG. 1. Schematic of the experiment showing the major beam line components (including the undulator source, spherical grating monochromator, and beam line optics) and our vacuum chamber end station (containing the double pinhole spatial filter, liquid crystal film, and detectors).

second pinholes, L is the distance between them, and λ is the wavelength. In our experiment $P_1 = P_2 = 35 \mu\text{m}$, $L = 37 \text{ cm}$, and $\lambda = 44 \text{ \AA}$. Light coming out of the second pinhole is then spatially coherent with a transverse coherence length equal to $35 \mu\text{m}$. The transverse coherence of the beam was directly verified experimentally by measuring and quantitatively fitting the Airy pattern observed when the sample was removed. The longitudinal coherence length is $\lambda(E/\Delta E) \approx 44 \mu\text{m}$. The maximum path length difference in the Bragg scattering geometry is approximately $2\mu^{-1} \sin(\theta_B)$, where μ is the absorption coefficient of the sample, and θ_B is the Bragg angle. In our experiments, $\mu^{-1} \approx 5 \mu\text{m}$, and $\theta_B \approx 50^\circ$. This gives a maximum path length difference of about $8 \mu\text{m}$, well below the maximum allowed path length difference of $44 \mu\text{m}$. After the multilayer was installed, our typical coherent fluxes were 3×10^8 photons/sec. Note that this is about 10^3 times less than that predicted by Eq. (1) due to the losses in the beam line optics, monochromator, and multilayer reflector. If it were not for the $2000\times$ increase provided by the use of soft x rays, we could not have done our experiments. The solution to this problem of losses is the same as that eventually arrived at by the hard-x-ray scatterers: to eliminate the beam line optics [3].

The freely suspended SmA film was held in a temperature controlled oven which was mounted on a rotation axis. A pass hole in the oven allowed the transmitted beam to be monitored with a detector downstream of the sample. This allowed us to continuously monitor the intensity noise in the incident beam. The Bragg reflected light was measured with a detector located 35 cm below the sample, near $2\theta = 100^\circ$. Since all of the SmA materials we studied have layer spacings near 30 \AA , the Bragg angle was nearly independent of the specific liquid crystal. A $50 \mu\text{m}$ pinhole was used in front of the Bragg detector so that a single coherence area of the scattered light was collected. In our detectors we used yttrium aluminum perovskite doped with cerium (YAP:Ce) scintillators to convert the soft x rays into ultraviolet light, which was then detected by a photomultiplier tube (PMT). Using a calibrated soft-x-ray photodiode, we measured the quantum efficiency of our detector to be about 50%. YAP:Ce was chosen because of its fast scintillation decay (25 ns for YAP:Ce versus 300 ns for NaI:Tl), and also because its light output (about 25% of NaI:Tl) was large enough to give us good quantum efficiency without giving us multiple counts for each soft-x-ray photon detected. The detector outputs were amplified, discriminated, and fed into a two-channel, logarithmic time base, digital correlator. This correlator calculated the time autocorrelation function of both the scattered and the transmitted intensities in real time. These correlation functions were then fit to the form shown in Eq. (2) below. Our count rates on the Bragg peak were typically about 10^6 detected photons per second.

An example of our raw data is shown in Fig. 2. Figure 2a compares the measured intensity-intensity correlation function of the scattered beam (thick line) with

that of the transmitted beam (thin line). Both correlation functions show afterpulsing effects at times faster than $1 \mu\text{s}$, intensity noise due to the pulsed nature of the electron storage ring in the range from about $1\text{--}10 \mu\text{s}$, and slower, periodic intensity modulations with periods of several tens of milliseconds resulting from additional intensity and angle noise in the incident beam. Figure 2b shows the corresponding normalized curve, calculated by dividing the scattered correlation function by the transmitted correlation function. The transmitted beam is composed mainly of unscattered light, and consequently it should not show the liquid crystal fluctuations, but it should show the correlated intensity noise in the incident beam. The normalization divides out the correlated intensity noise in the incident beam, leaving only the contribution from the thermally driven liquid crystal layer fluctuations. Note that this normalization works well in the time range from about $1 \mu\text{s}$ to 1 ms . Afterpulsing effects presently limit us to times slower than about $1 \mu\text{s}$. This is also the limit for conventional laser light scattering using PMTs which exhibit afterpulsing. Also note that part of the slower periodic noise is not normalized. We attribute this to angle noise in the incident beam which is converted into intensity noise in the scattered beam due to the angular selectivity of the Bragg reflection. Presently, this lower frequency noise limits us to times faster than a few milliseconds.

Both the normalized and the unnormalized scattered intensity-intensity correlation functions are fit very well by the exponential form

$$\langle I(t)I(0) \rangle = B + A \exp(-t/\tau). \quad (2)$$

Here, the angular brackets indicate the time average, and the three parameters (the decay time τ , the amplitude A , and the base line B) were varied in our nonlinear least

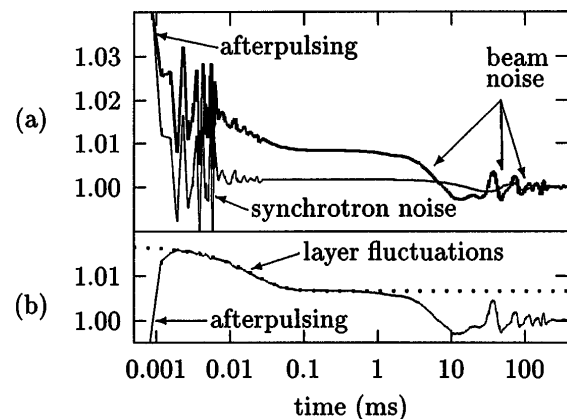


FIG. 2. Comparison of the measured intensity-intensity correlation function before and after normalization. (a) The unnormalized correlation functions of the scattered (thick line) and transmitted (thin line) beams. (b) The normalized correlation function calculated by dividing the scattered correlation function by the transmitted beam correlation function. The dotted line is a fit to Eq. (2).

squares fits. The decay times τ were found experimentally to vary both with the liquid crystal material and with the thickness of the film. The amplitude A varied with the level of coherence and with the scattering wave vector. The base line B varied with the amount of angle noise in the beam and was not under our control.

For films thicker than about $20 \mu\text{m}$, the soft-x-ray transmission was so low that we could not measure the transmitted beam. In these cases, we fit the unnormalized Bragg intensity-intensity correlation function directly. In order to test for systematic errors resulting from the unnormalized synchrotron bunch noise (in the time range $1\text{--}10 \mu\text{s}$), we fit both the normalized and the unnormalized data whenever possible. However, we found that our fits to the unnormalized Bragg correlation functions gave results indistinguishable from our fits to the normalized correlation functions. This is because the noise added by the ring bunches is very regular and because it is small over much of the range of fitting data. All of the results reported here are from fits to unnormalized correlation functions in order to apply the same analysis technique to all of our data. We have described our work with normalization because we believe that it will become more important at faster times than we have measured in our present experiment. Faster times will be accessible in future experiments using raw undulator light and low after-pulsing photomultipliers.

Our main experimental results are summarized in Fig. 3, where we plot the measured decay time vs the measured film thickness for the five liquid crystals that we studied. Note that there is an obvious linear dependence of the decay time on the film thickness. Each film thickness was determined by measuring the soft-x-ray transmission of the film and then converting the transmission to a thickness using the absorption coefficients for the liquid crystals as calculated using the on-line program available at the Center for X-Ray Optics website [7]. The experimental uncertainties are dominated by the uncertainty in the absorption lengths, which is due to the uncertainties in the photon energy and the liquid crystal density. This uncertainty in the absorption length translates into a 10% uncertainty in the film thickness measurements.

The detailed microscopic theory for our results has been reported elsewhere [8]. In general, the dynamics depend on the layer compression modulus B , the layer bending rigidity K , the surface tension γ , and the layer sliding viscosity η_3 . However, simple arguments and the detailed calculations presented in Ref. [8] both show that, for our present experiment, the equations of motion can be simplified considerably. Because we are making our measurements centered on the Bragg peak, we are most sensitive to fluctuations with a transverse wavelength equal to our transverse x-ray coherence length, $35 \mu\text{m}$. For these fluctuations, the bending rigidity terms can be neglected because they are small, and the layer compression terms can also be neglected because the compression stiffness is so large that the simple approximation that all

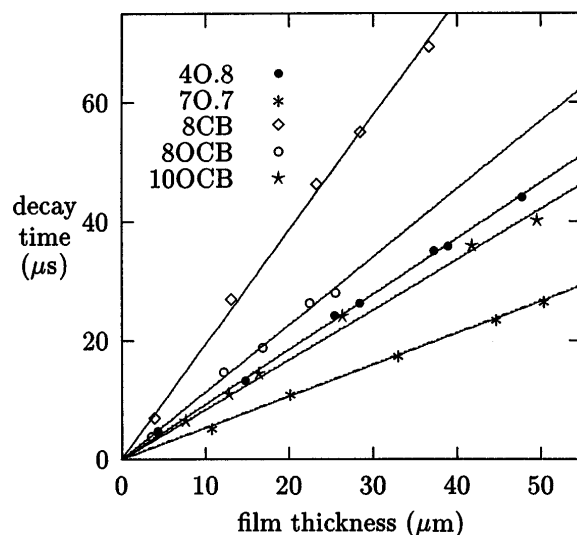


FIG. 3. Plot of decay time versus film thickness for the liquid crystals studied in this experiment. The measured standard deviations are about $1 \mu\text{s}$ for the decay times, and about $1 \mu\text{m}$ for the thicknesses. The straight lines are fits to the theoretical predictions given by Eq. (3).

the layers move together is valid. In this limit, the dispersion relation leads to the following form for the decay time of the modes:

$$\tau = \left(\frac{\eta_3}{2\gamma} \right) L. \quad (3)$$

Here, L is the thickness of the film. Note that the decay time is independent of the transverse wave number of the fluctuations. We point out that although the fluctuations we detect are dominated by those with a transverse wavelength near $35 \mu\text{m}$, the parallel (along the layer normal) component of the momentum transfer is $2\pi/d \approx 2 \times 10^6 \text{ cm}^{-1}$. This wave vector is about 100 times larger than that accessible with laser DLS. If the layers were fluctuating independently, we would measure a deviation from Eq. (3) due to the contribution from the layer compression modes. Consequently, our experiment demonstrates that the layers are moving together.

The complete theoretical calculation of the Bragg peak intensity-intensity correlation function that we have measured is very difficult because it involves the numerical evaluation of a complicated 10-dimensional integral for every delay time [8]. So, instead, in order to estimate this correlation function and relate it to the theory discussed above, we did a simple Monte Carlo (MC) simulation of the equation of motion derived in Ref. [8]. Our MC simulations show that the thermally driven fluctuations in the film cause the scattered Bragg intensity to have a small, fluctuating component, in addition to a large static component. The small fluctuations in the Bragg intensity are due to fluctuations in the film which have a transverse wavelength equal to our transverse x-ray coherence length, $35 \mu\text{m}$. The autocorrelation function of the simulated Bragg peak intensity is of the form given in Eq. (2), and the decay time is given by Eq. (3).

To analyze our results, we fit the data shown in Fig. 3 to Eq. (3). Our data clearly show the linear dependence of decay time vs thickness that is predicted by theory. To test the theory more completely, independent measurements of the layer sliding viscosities η_3 must be made. However, if we assume that the theory is correct, which is consistent with the linear dependence of the decay time on the thickness, we can calculate η_3/γ values for each of the five liquid crystals studied in this experiment. The results are shown in Table I. The top two rows of the table contain our data for the two monolayer smectics we studied (4O.8, 7O.7), and the bottom three rows contain our results for the three bilayer smectics we studied (8CB, 8OCB, 10OCB). For all but one of the liquid crystals in this study, the surface tension γ is known [9], and so we can calculate the layer sliding viscosity η_3 . For 10OCB, we could not find any measurement of the surface tension in the literature, so we estimated η_3 for 10OCB by using the fact that many similar bilayer SmA liquid crystals have a surface tension of about 27 dyn/cm [9]. In the case of 8CB, we were able to find two previous measurements of the layer sliding viscosity which used two different experimental methods [10,11]. The results from these experiments are the following: (1) 1.0 ± 0.2 poise at 28 °C for Ref. [10], and (2) 1.2 poise (uncertainty unreported) at 30 °C for Ref. [11]. These independent measurements are in excellent agreement with our own value of 1.0 ± 0.1 poise measured at 27.9 °C.

In conclusion, our experiment demonstrates the utility of soft-x-ray DLS in studies of microsecond fluctuations on molecular length scales. The use of the Bragg peak to concentrate all of the counts into one “spot” in reciprocal space makes the study of microsecond fluctuations possible with an input intensity of only 3×10^8 photons per second. We are studying time scales as fast as most visible light DLS. We have also shown that normalization can be used to eliminate the pure intensity noise due to the inherent pulsed nature of synchrotron beams. Our experiment is a step toward the wonderful possibilities offered by fast-time x-ray DLS, which promises direct access to the dynamics of condensed matter and biological systems on time and length scales not readily accessible with any other techniques.

In our future work we intend to study the undulation modes of smectics by measuring the fluctuations in the scattering away from the Bragg peak. It is the divergence of the thermally excited amplitude of the undulation modes which leads to the destruction of the long-range order in this system—as was first predicted theoretically by Caillé [12], and later confirmed in a number of elegant incoherent x-ray scattering experiments [13–15]. In our studies, we will measure the time scales

TABLE I. Summary of our experimental results. The first column lists the liquid crystal (LC) material. The second column shows the values derived from the slopes of fits to data shown in Fig. 3. The known values for the surface tension γ are given in column three. These γ values are used to calculate the layer sliding viscosity η_3 . The fifth column gives the temperature at which the data was taken.

LC	η_3/γ (sec/m)	γ (dyn/cm)	η_3 (poise)	T (°C)
4O.8	1.85 ± 0.19	21.0	0.39 ± 0.04	54.5
7O.7	1.07 ± 0.11	21.0	0.22 ± 0.02	75.5
8CB	3.82 ± 0.40	26.5	1.0 ± 0.1	27.9
8OCB	2.28 ± 0.23	27.0	0.62 ± 0.06	58.1
10OCB	1.69 ± 0.17	(27)	(0.46)	64.1

of these same fluctuations. This work will be made possible by two simple technical improvements: (1) increasing our coherent flux by 1000 times by using the raw light from an undulator (thus avoiding the losses in the beam line optics), and (2) improving our time resolution to tens of nanoseconds by using low afterpulsing PMTs and a faster digital correlator.

Financial support from the U.S. Department of Energy under Grant No. DE-FG06-86ER45275, from the American Chemical Society Petroleum Research Fund, from the University of Washington Molecular Biophysics Training Grant, from KBN Grants No. 3T09A07212 and No. 2P03B12516, and from the Maria Skłodowska Curie Joint Fund II is gratefully acknowledged. This work was carried out in part at the Advanced Light Source at Lawrence Berkeley National Laboratory, which is supported by the U.S. Department of Energy.

- [1] S. B. Dierker *et al.*, Phys. Rev. Lett. **75**, 449 (1995).
- [2] T. Thurn-Albrecht *et al.*, Phys. Rev. Lett. **77**, 5437 (1996).
- [3] S. G. J. Mochrie *et al.*, Phys. Rev. Lett. **78**, 1275 (1997).
- [4] S. Brauer *et al.*, Phys. Rev. Lett. **74**, 2010 (1995).
- [5] K. Kim, Nucl. Instrum. Methods Phys. Res., Sect. A **246**, 71 (1986).
- [6] *X-Ray Data Booklet*, edited by D. Vaughan (Lawrence Berkeley Laboratory, University of California, Berkeley, CA, 1986).
- [7] http://www-cxro.lbl.gov/optical_constants
- [8] A. Poniewierski *et al.*, Phys. Rev. E **58**, 2027 (1998).
- [9] P. Mach *et al.*, J. Phys. II (France) **5**, 217 (1995).
- [10] P. Oswald (private communication); J. Phys. (Paris) **47**, 1091 (1986).
- [11] C. Baumann *et al.*, Phys. Rev. Lett. **54**, 1268 (1985).
- [12] A. Caillé, C. R. Acad. Sci. Ser. B **274**, 891 (1972).
- [13] J. Als-Nielsen *et al.*, Phys. Rev. Lett. **39**, 1668 (1977); J. Als-Nielsen *et al.*, Phys. Rev. B **22**, 312 (1980).
- [14] C. R. Safinya *et al.*, Phys. Rev. Lett. **57**, 2718 (1986).
- [15] R. Zhang *et al.*, Phys. Rev. Lett. **74**, 2832 (1995).